Dental Materials Journal 2017; 36(4): 503–510

Antimicrobial and antibiofilm activities of MTA supplemented with bismuth lipophilic nanoparticles

Rene HERNANDEZ-DELGADILLO[1], Casiano DEL ANGEL-MOSQUEDA[1], Juan Manuel SOLÍS-SOTO[1], Silvia MUNGUIA-MORENO[2], Nayely PINEDA-AGUILAR[3], Rosa Isela SÁNCHEZ-NÁJERA[1], Shankararaman CHELLAM[4] and Claudio CABRAL-ROMERO[1]

[1] *Dental School, Autonomous University of Nuevo Leon, UANL, Monterrey, Nuevo Leon, Mexico*
[2] *Odontological Sciences, School of Stomatology, Autonomous University of San Luis Potosi, UASLP, San Luis Potosi, Mexico*
[3] *Advanced Materials Research Center, CIMAV Unidad Monterrey, Nuevo Leon, Mexico*
[4] *Texas A & M University, College Station, TX, USA*
Corresponding author, Claudio CABRAL-ROMERO; E-mail: claudio.cabralrm@uanl.edu.mx

The objective of this work was to determine the antimicrobial and antibiofilm properties of mineral trioxide aggregate (MTA) supplemented with bismuth lipophilic nanoparticles (BisBAL NPs). The antimicrobial activity of the composite MTA-BisBAL NPs was determined by the disk diffusion assay, while antibiofilm activity was analyzed by fluorescence microscopy. The cytotoxicity of MTA-BisBAL NPs was determined on human gingival fibroblasts by optical microscopy and crystal violet staining. MTA-BisBAL NPs inhibited the growth of *Enterococcus faecalis*, *Escherichia coli*, and *Candida albicans* and also detached the biofilm of fluorescent *E. faecalis* after 24 h of treatment. The addition of BisBAL nanoparticles did not significantly modify the physical properties of MTA, and cytotoxicity was not observed when MTA-BisBAL NPs was added on human gingival fibroblasts. Altogether these results suggest that BisBAL nanoparticles provide antimicrobial and antibiofilm activities to MTA while it retained their biophysical properties without cause side effects on human gingival fibroblasts.

Keywords: Antimicrobial activity, Antibiofilm activity, Bismuth nanoparticles, Mineral trioxide aggregate

INTRODUCTION

Mineral trioxide aggregate (MTA) is one of most common biomaterials used in endodontic treatment based on its good biological action and tissue repair obtaining good results since 1990s[1)]. The major component, Portland cement is a mixture of dicalcium silicate, tricalcium silicate, tricalcium aluminate, gypsum, and tetracalcium aluminoferrite[2)]. Early reports described antimicrobial activity of MTA[1,3)], however their level was very poor requiring until 50 mg/mL to inhibit the microbial growth. Failure in endodontic treatment is not weird and the usual factors for this are: *persistence bacteria*, inadequate filling of the canal, improper coronal seal, untreated canals, *etc*. *E. faecalis* biofilm on root canal, dentinal tubules and ramifications is not always eradicated during treatment may due to low time of exposition to disinfectants. It is urgent the developing new biomaterials with antimicrobial and antibiofilm activities to fight successfully endodontic infections.

Nanotherapeutics hold promise to revolutionize medical treatment with potent, smart, and less toxic drugs[4)]. To date research has largely focused on metal nanoparticles (NPs) made from silver, gold, zinc, and titanium which have been reported to display good antimicrobial activity[5)]. However, most of them are also potentially toxic, limiting their use in humans[6)]. In contrast, bismuth is non-carcinogenic and less bioaccumulative and cytotoxic[7-9)] consequently being often referred to as a "green" element. To date, soluble and nanoparticulate bismuth compounds have been evaluated as antimicrobial agents in many biomedical and environmental systems[10-14)], but their use in dentistry field has not been evaluated. In previous reports we have described the antimicrobial and antibiofilm activities *in vitro* of lipophilic bismuth nanoparticles (BisBAL) against oral microorganisms growth[15)] and the absence of cytotoxicity on human epithelial and blood cells[16,17)].

The aims of this study were to: i) synthesize and characterize BisBAL nanoparticles, ii) develop a MTA supplemented with BisBAL NPs and evaluate their antimicrobial and antibiofilm activities, iii) determine mechanical properties and surface characteristics of the new composite MTA-BisBAL NPs and compare them with the native MTA, and iv) analyze the cytotoxicity of MTA-BisBAL NPs employing primary culture of human gingival fibroblasts.

MATERIALS AND METHODS

A general description of the methodology employed is illustrated at Fig. 1.

Microbial culture

Enterococcus faecalis, Escherichia coli and *Candida albicans* growth (ATCC numbers; 11420, 25922 and 90029) were cultured in trypticase soy broth agar (TSB; BD DIFCO, Sparks, MD, USA) at 37°C for 24 h in aerobic

Color figures can be viewed in the online issue, which is available at J-STAGE.

Received Jul 22, 2016: Accepted Dec 19, 2016
doi:10.4012/dmj.2016-259 JOI JST.JSTAGE/dmj/2016-259

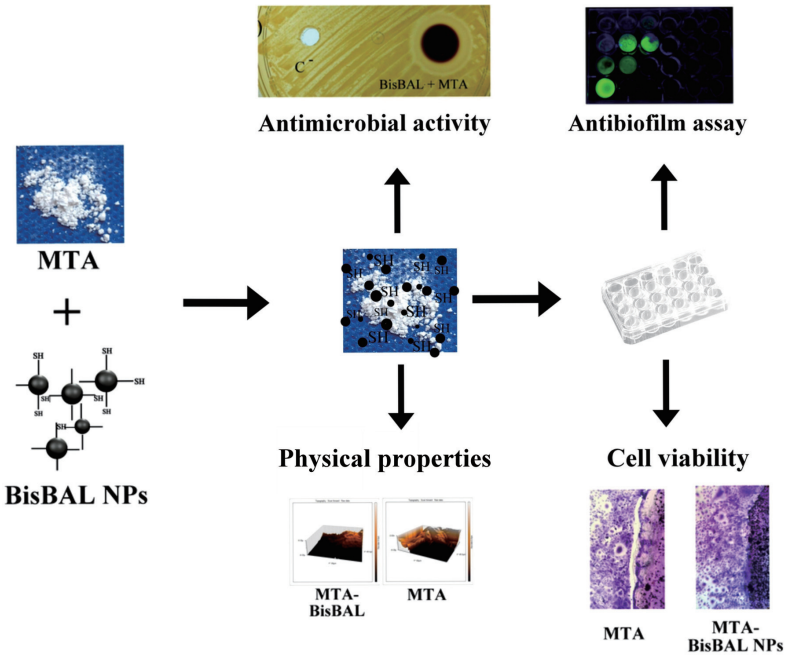

Fig. 1 Lipophilic bismuth nanoparticles (BisBAL NPs) have an important antimicrobial and antibiofilm efficacy.
The objective of this study was to determine the antimicrobial-antibiofilm and physical properties of mineral trioxide aggregate (MTA) supplemented with bismuth lipophilic nanoparticles (BisBAL NPs) such as citotoxicity.

conditions. Exponential phase microorganisms were employed to antimicrobial and antibiofilm experiments.

Synthesis and characterization of BisBAL nanoparticles
BisBAL nanoparticles were synthesized and characterized as early was described in previous publications[15]. Briefly, bismuth (Bis) was mixed with 2,3-dimercapto-1-propanol (BAL) in a molar ratio 2:1 and the resultant composite BisBAL was reduced by sodium borohydride to generate BisBAL NPs. The stock suspensions of 25 mM of BisBAL NPs in 10 mL batches were prepared and stored at 4°C until use. Information on the shape and size of nanoparticles was obtained using scanning electron microscopy (SEM; FEI Tecnai G2 Twin, FEI, Hillsboro, OR, USA; 160 kV accelerating voltage). The rhombohedral crystallinity and crystallite size were determined using the X-ray diffractometer (XRD; X'Pert PRO MRD PANalytical, Lelyweg, The Netherlands) equipped with Cu Kα as X-ray source (λ=1.541874 Å). Diffractograms were interpreted using the Debye-Sherrer formula (X'Pert Data Viewer software PANalytical, Lelyweg, The Netherlands) to estimate the rhombohedral structure and crystallite size.

MTA-BisBAL NPs mixture preparation
MTA was freshly prepared following manufacturer instructions (Angelus, Londrina, BA, Brazil). Employing a sterile glass slab, 1 spoon (≈140 mg) of MTA was mixed with 50 µL of BisBAL nanoparticles to get a final concentration of 10 mg/mL. All mixtures were fresh prepared before each experiment.

Antimicrobial activity of MTA-BisBAL NPs
The antibacterial and antifungal activities of MTA-BisBAL NPs on *Enterococcus faecalis, Escherichia coli* and *Candida albicans* growth were determined by the Kirby and Bauer disk diffusion method[18]. Microorganisms were grown in trypticase soy broth agar (TSB, BD DIFCO) at 37°C, overnight in aerobic conditions with standard inoculums (0.5 MacFarland). One hundred microliter of bacteria culture was spread on TSB agar plates using a sterile cotton swab. Then, wells were punched with a previously sterilized 5 mm diameter polyestyrene ring. MTA-BisBAL NPs were embedded into the agar plate to interfere with bacterial growth. MTA alone was employed as a negative control and after overnight incubation at 37°C the halo diameter was measured with a vernier. Bactericidal and antimycotical assays were carried out in triplicate to assess the veracity of results.

Antibiofilm activity of MTA-BisBAL NPs against fluorescent E. faecalis biofilm
The anti-biofilm properties of MTA-BisBAL NPs were determined by adding it to recombinant-fluorescent *E. faecalis* biofilm of 24 h formed. To the bacterial biofilm

was added 2% agar-gels pellets with BisBAL NPs (10 mg/mL), MTA (10 mg/mL) and mix MTA-BisBAL NPs- (5-5 mg/mL). As a positive control 2.62% NaOCl was used (Corning-Costar, Corning, NY, USA). Cells were maintained in culture media for 24 h. Finally, the medium was removed and the cells were washed three times with phosphate buffered saline (PBS). The remain cells into the biofilm after treatments were quantified measuring the fluorescence intensity using a 12-well scanning fluorometer GloMax® Multi+Micoplate Multimode (Promega, Madison, WI, USA) at 525 nm. Data were analyzed to determine the number of viable cells and the experiment was done by triplicate to assess the veracity of results.

Microhardness and surface roughness of MTA-BisBAL NPs

To determine whether addition of bismuth nanoparticles could change the mechanical properties of MTA, the microhardness and surface roughness were analyzed[19,20]. Disks of 5 mm of diameter and 2 mm of depth of MTA and MTA-BisBAL NPs were employed. The Vickers hardness test was employed to measure the microhardness (Micro Vickers Hardness Tester HV-1000, DongGuan Sinowon Precision Instrument, South District DongGuan, China). A diamond indenter was used with a load of 300 g for 15 s. Each sample was submitted to 3 indentations separated by 200 μm. The microhardness value is expressed as the average of 3 individual measurements (*i.e.* triplicate measurements were made). Surface roughness measurements were carried out at a scanning rate of 49.5 μm/s using atomic force microscopy (AFM, Nanosurf Easy Scan 2, SPM Electronics, Liestal, Switzerland) in the contact mode with a silicon nitride (SiN) probe. The conditions used for the short cantilever contact mode were as follows: spring constant, 0.1 N/m; resonant frequency, 28 kHz; length, 225 μm; mean width, 28 μm, thickness, 1 μm; tip height, 14 μm; radius, <10 nm. The Nanosurf Easy Scan 2 software (Version 1.6) was used to analyze data. The feedback gains with a set point of 20 nN were as follows: P-Gain: 10,000; I-Gain: 1,000; and D-Gain: 0. A calibration grid silicon oxide on silicon material (Nanosurf AG, CH-4410, SPM Electronics) with an XY periodicity of 10 μm and a Z height of 119 nm was used for calibration prior to each evaluation session. All samples were evaluated at the same scan size (49.5×49.5 μm^2) in triplicate and in different areas, selected at random.

Cell culture and fluorimetric cytotoxicity assay

Human gingival fibroblasts (HGF) were cultivated in Dulbecco's modified Eagle's medium (DMEM)/Ham's F12 (DMEM/F12) supplemented with 10% fetal bovine serum (FBS) (Gibco-Invitrogen, Carlsbad, CA, USA) and 100 U/mL penicillin, 100 μg/mL streptomycin and 0.25 μg/mL amphotericin B (Sigma-Aldrich, St. Louis, MO, USA) at 37ºC in a humidified atmosphere with 5% CO_2[21]. After obtaining cell confluence, ~8×10^4 per well were seeded onto 12-well plates containing 2% agar-gels pellets with BisBAL NPs (10 mg/mL), MTA (10 mg/mL) and mix MTA-BisBAL NPs- (5-5 mg/mL). As a positive control 2.62% NaOCl was used (Corning-Costar). Cells were maintained in growth medium for 24 h. Finally, the medium was removed and the cells were washed three times with phosphate buffered saline (PBS). The cytotoxicity assay was performed as described by Larsson and Nygren[22]. Briefly, fluorescein diacetate (FDA, Sigma-Aldrich) was dissolved in DMSO (Sigma-Aldrich) and kept frozen at −20ºC as a stock solution (10 mg/mL). FDA was diluted in PBS at 10 μg/mL and 1 mL was added to each well. The plates were then incubated for 30 min at 37ºC in the dark. A 12-well scanning fluorometer GloMax® Multi+Micoplate Multimode (Promega) was used at 495 nm. Data were analyzed to determine the number of viable cells.

Statistical analysis

D'Agostino-Pearson K^2 test used to assess normality of data. Analysis of Variance (ANOVA) and student's *t* tests used to evaluate the treatments effects, and Dunnett's test for differences between treatments and control groups. All statistical tests, significance level of α=0.05 was considered.

RESULTS

Characterization of BisBAL Nanoparticles

Individual bismuth nanoparticles synthesized were largely spherical in shape with a number-weighted average hydrodynamic diameter of 29.3 nm but were aggregated tightly into larger clusters as can be seen in SEM images (Fig. 2A). The identity of bismuth was corroborated by its EDX (Fig. 2B) spectrum and X-ray diffraction pattern (Fig. 2C).

Antimicrobial activity of MTA-BisBAL NPs

As expected from our previous reports[15,23], BisBAL nanoparticles showed a high antimicrobial activity against all microorganisms tested (Figs. 3A–D). The average halo diameter of 100 mg/mL of BisBAL NPs for *E. faecalis* was 19 mm, *E. coli* 24 mm and *C. albicans* 23 mm, while for a mixed culture was 18 mm. Fresh mixture of MTA with BisBAL NPs was analyzed to interfered with microbial growth and as seen in Figs. 3E–H, MTA supplemented with 100 mg/mL of BisBAL NPs did indeed inhibit bacterial and fungal growth, individually and for mixed cultures. The average halo diameter of MTA-BisBAL NPs was 23 nm for *E. faecalis*, 21 mm for *E. coli* and 24 mm for *C. albicans*, while it was 22 mm for a mixed culture. MTA alone did not inhibit the microbial growth as can be observed in each petri plate. These results strongly suggest that BisBAL nanoparticles provide effective bactericidal and antimycotical properties to MTA.

Antibiofilm activity of MTA-BisBAL NPs on fluorescent E. faecalis biofilm

Based on earlier results described above we focused in determine if the mixture MTA-BisBAL NPs could also present antibiofilm activity. To evaluate this property,

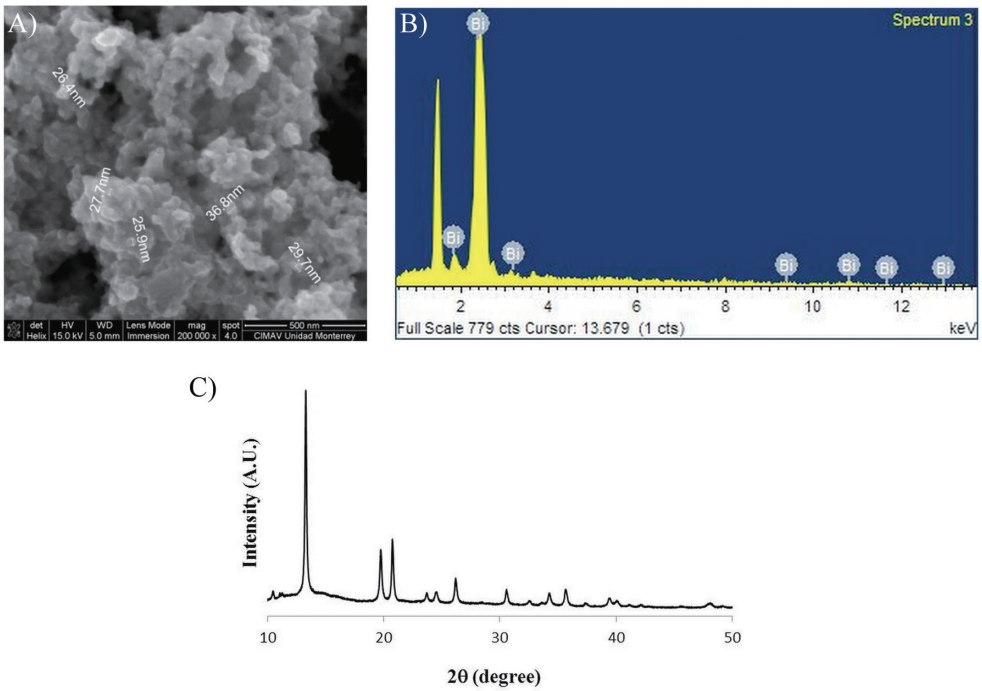

Fig. 2 BisBAL NPs visualized by scanning electron microscopy (SEM).
A) The dominant population of spherical shaped nanoparticles (<100 nm), showed the NPs clusters interspersed among the lesser electron dense material is shown in the SEM images. B) EDS spectrum showed the element composition in the sample observed by SEM. C) The bismuth presence in the sample of BisBAL nanoparticles was identified by X-ray diffraction pattern.

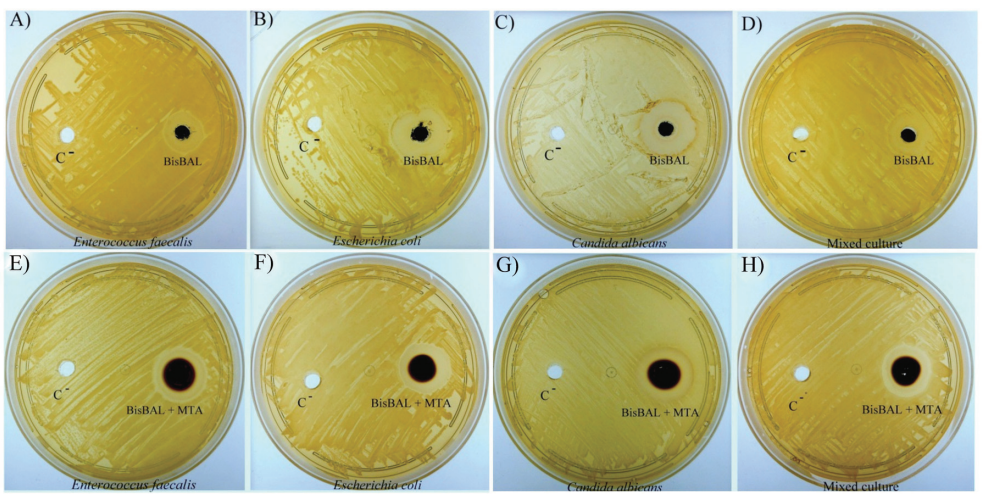

Fig. 3 Bactericidal and antimycotic activities of BisBAL NPs and MTA-BisBAL NPs.
A–D) The growth of both the individual and mixed cultures of *Enterococcus faecalis*, *Escherichia coli*, and *Candida albicans* were inhibited by BisBAL NPs (100 mg/mL). E–H) MTA-BisBAL NPs inhibiting the bacterial growth. The halo diameter around disk filters impregnated.

we used a fluorescent recombinant strain of *E. faecalis*. A 24 h biofilm old of fluorescent *E. faecalis* was exposed to BisBAL nanoparticles, MTA, mixture of MTA-BisBAL NPs or hypochlorite for 24 h and the remain biofilm was observed and quantified. The results showed a complete detachment of the biofilm after treatment with BisBAL NPs in comparison with the growing control ($p<0.001$) (Fig. 4A). In contrast MTA alone looks similar to the

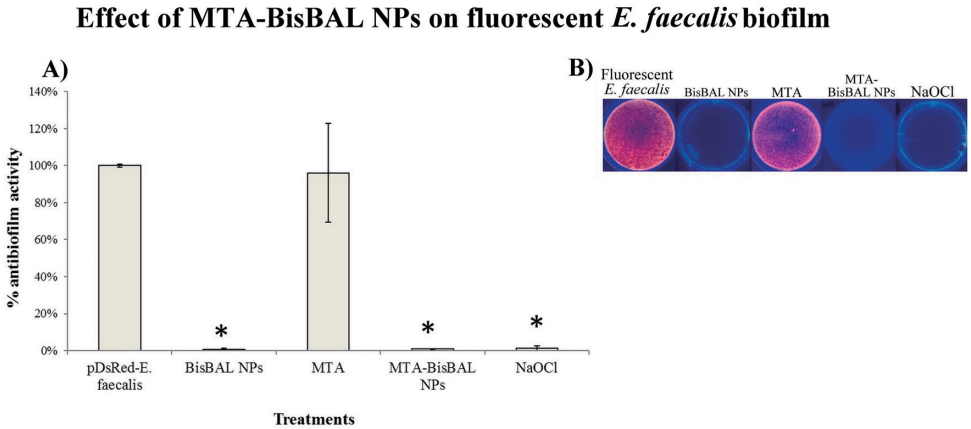

Fig. 4 Antibiofilm activity of MTA-BisBAL NPs against fluorescent *Enterococcus faecalis* biofilm.
A) To the bacterial biofilm was added 2% agar-gels pellets with BisBAL NPs (10 mg/mL), MTA (10 mg/mL) and mix MTA-BisBAL NPs- (5-5 mg/mL). As a positive control 2.62% NaOCl was used. The remaining cells into the biofilm after treatments were quantified measuring the fluorescence intensity using a 12-well scanning fluorometer GloMax® Multi+Micoplate Multimode. B) *E. faecalis* biofilm florescence was observed by using an UV-transiluminator. Antibiofilm activity was significantly reduced with MTA-BisBAL NPs treatment compared to all groups (*p<0.001). Error bars indicate mean±SD (n=4), asterisk indicate statistical differences (α=0.05).

Table 1 Summary of physical properties

	Material			
	MTA alone	MTA-BisBAL NPs composite	Student's t test	p
Microhardness	36.96±13.975	22.73±4.085	1.6933	0.16566
Surface roughness	122.44±45.285	87.12±26.792	1.1624	0.309704

Values indicate mean±SD (n=4). Considering a significance level of α=0.05.

growing control lacking antibiofilm activity, while mixture MTA-BisBAL NPs detached the biofilm with same efficacy than BisBAL NPs alone (p<0.001) (Fig. 4A). As inhibition control was employed hypochlorite and no biofilm was detected after 24 h. The fluorescence intensity measured showed 0% of biofilm in the treatments with BisBAL NPs, MTA-BisBAL NPs and hypochlorite in comparison with growing control taken as 100% (p<0.001) (Fig. 4B). Altogether these results suggest that BisBAL nanoparticles confer antibiofilm activity to MTA, inhibiting the biofilm of fluorescent *E. faecalis*.

Physical properties of MTA- BisBAL NPs

The microhardness of MTA was measured to be 36.9±13.9 for MTA and 22.7±4.1 for MTA-BisBAL NPs composite (Table 1). The surface roughness of MTA was 122.43±45.3 and 87.1±26.7 for MTA-BisBAL NPs (Table 1). Representative 3-D images of the surfaces of MTA-BisBAL NPs and MTA alone are given in Fig. 5. Statistical analysis demonstrated no significant differences in the average microhardness (p=0.165) or surface roughness (p=0.309) demonstrating that addition BisBAL NPs did not change the physical properties of MTA.

Cytotoxicity of MTA-BisBAL NPs on human gingival fibroblasts

Since MTA has been modified by adding bismuth nanoparticles, we decided to analyze its possible cytotoxicity on human gingival fibroblast (HGF) for 24 h by optical microscopy. Figure 6A shows a clear adherence of HGF cells to BisBAL nanoparticles alone and to the mixture MTA-BisBAL NPs lacking cytopathic signs and looking very similar to the growing control (p<0.001). In contrast, hypochlorite kills all cells around it detecting no-living cells in comparison with the growing control (p<0.001). Interestingly BisBAL nanoparticles seems

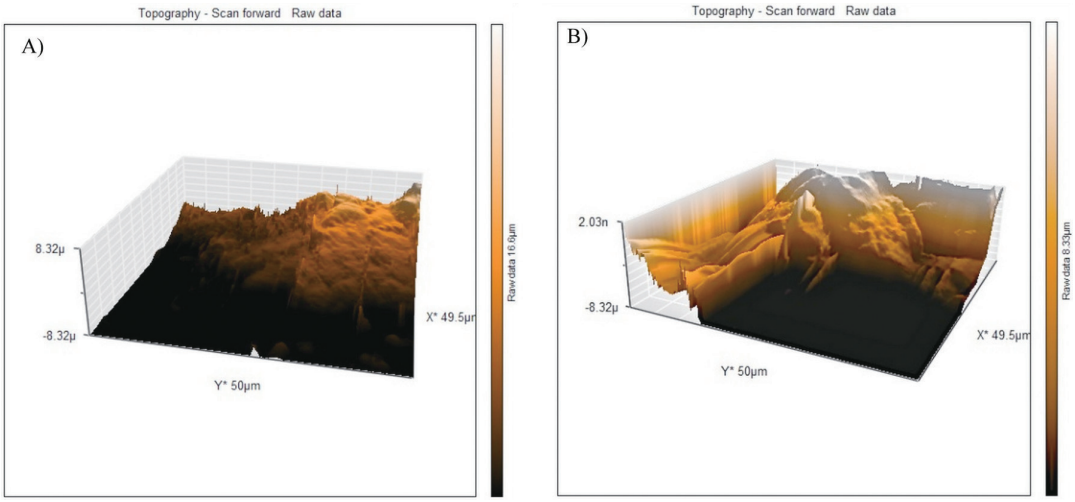

Fig. 5 Surface roughness of MTA-BisBAL NPs employing atomic force microscopy. 3D images of MTA-BisBAL (A) and MTA alone (B).

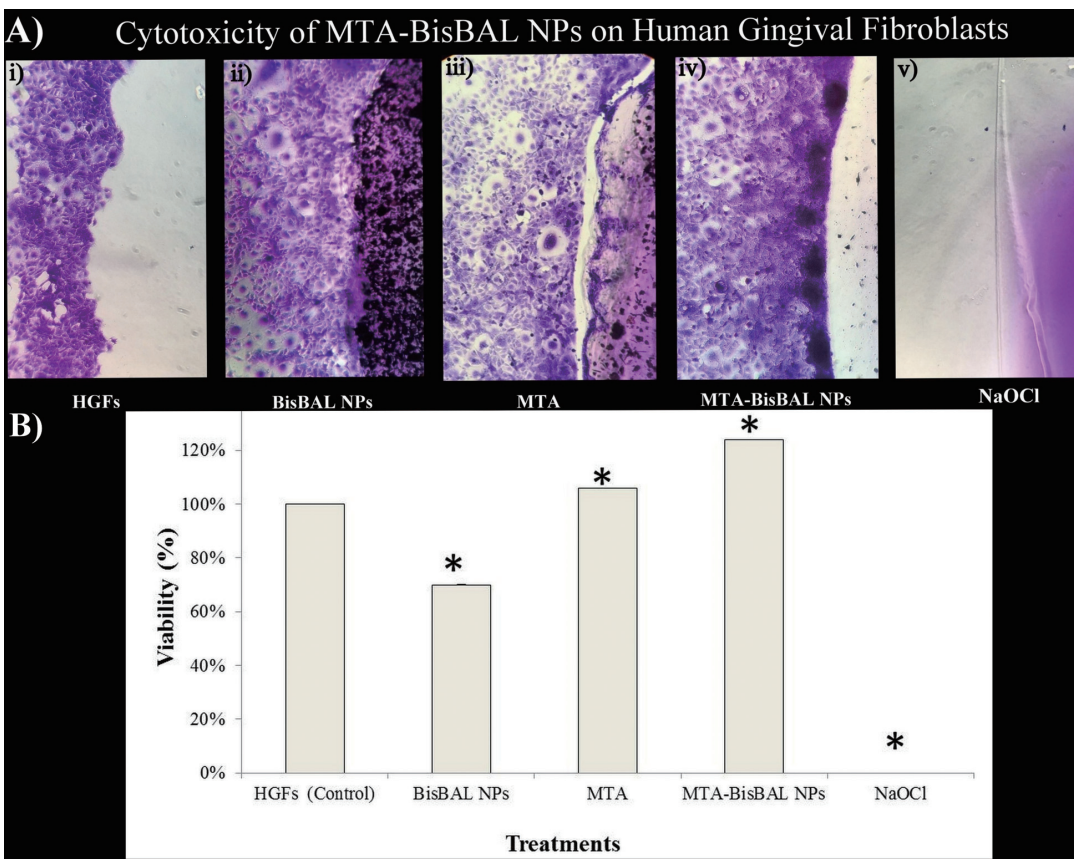

Fig. 6 Cytotoxicity of MTA mixed with BisBAL NPs on human gingival fibroblasts (HGF). A) A confluent monolayer of HGFs was exposed to BisBAL nanoparticles, MTA, MTA-BisBAL NPs or sodium hypochlorite for 24 h. After treatment cells were stained with crystal violet and observed using an inverter optic microscope. HGFs growing in culture media were used as growing control. B) The experiment described above was used to measure the number of living cells after treatment. Cell viability of HGFs was significantly increased with MTA-BisBAL NPs treatment compared to all groups (*p<0.001). Asterisk indicate statistical differences (α=0.05).

to attract to the cells may be due to its lipophilicity increasing the adherence of HGF to MTA in the mixture MTA-BisBAL NPs in comparison with MTA alone as can be seen in Fig. 6B ($p<0.001$). The cells presented a normal morphology, including a well-defined membrane and the absence of light refraction and rounding suggesting that MTA-BisBAL NPs cause not side effects on HGF cells.

DISCUSSION

To date several reports have been described antimicrobial properties of several metallic nanoparticles such as silver, gold, zinc, titanium and bismuth[24]. Nevertheless, medical applications employing these nanostructures are limited. In this manuscript, we show evidence about antimicrobial and antibiofilm properties of MTA supplemented with bismuth nanoparticles. Previous reports described a poor antimicrobial activity of MTA which vary depending of its composition[1]. Several medical devices have already been supplemented with nanocomposite hydrogels improving their mechanical and biological properties[25]. Nanoparticles as antimicrobials agents in endodontics have been increased in last 5 years[26]. Early reports show adhesives and composites supplemented with nanoparticles to provide bactericidal and remineralizing properties[27,28]. In this work we provide evidence of how MTA mixture with BisBAL nanoparticles (MTA-BisBAL NPs) acquired bactericidal and antimycotical activities in comparison with MTA alone. These results are agreed with the report of Estrela *et al*. who described the absence of antimicrobial activity in MTA alone[29]. Interestingly Tanomaru *et al*. reported antimicrobial activity of root canal sealer based on MTA (Endo CPM Sealer) and white MTA-Angelus against several oral pathogens including *Candida albicans* and *Enterococcus faecalis*[30]. Our results employing the same method (agar diffusion method) differ from Tanomaru data may be due a different composition among MTA and the variants used in that report. While Del Carpio-Perochena *et al*. described bactericidal activity of MTA supplemented with chitosan nanoparticles after prolonged aging[31]. The obtained results in this manuscript includes the antibiofilm activity of MTA-BisBAL NPs, which correlates with the early report of Wang *et al*. describing the antibiofilm activity of resin-modified glass ionomers supplemented with silver nanoparticles[32,33]. However bismuth nanoparticles have several advantages; are non-carcinogenic, less bioaccumulative and cytotoxic than other "heavy" metals including antimony, lead and silver[7,8,34]. The action mechanism through MTA-BisBAL NPs inhibit the microbial growth and biofilm formation is still unknown, but we hypothesize that the presence of bismuth nanoparticles into the mixture let a long-permanent exposition of BisBAL nanoparticles to oral pathogens inhibiting their growing and biofilm formation.

In order to analyze the physical properties of the new composite MTA-BisBAL NPs, microhardness and surface roughness were determined. Microhardness and surface roughness in MTA-BisBAL NPs decreased a little in comparison with MTA alone, which is consistent with previous reports analyzing physical properties of modified-cements[35,36]. When MTA was treated with EDTA the microhardness reduced significantly suggesting that EDTA interferes with hydration of MTA reducing hardness[36]. In our case BisBAL NPs addition cause the opposite effect on MTA developing a better composite.

When cytotoxicity of mixture MTA-BisBAL NPs and MTA alone was analyzed on human gingival fibroblasts (HGF) we found that BisBAL nanoparticles did not affect to HGF after 24 h of exposition. This result is consistent with the early report of Poggio *et al*. who described lack of cytotoxicity in MTA and biodentine[37]. Interestingly, MTA-BisBAL NPs seems to attract to HGF in comparison with MTA alone may be due to lipophilicity of BisBAL nanoparticles. Silver compounds and nanoparticles have already been used as dental restorative materials, endodontic retrofill cements, however their use in humans is limited due to their high toxicity[29].

In summary MTA-BisBAL NPs exhibited antimicrobial and antibiofilm activities without affecting the mechanical properties of native MTA. The mixture MTA-BisBAL NPs lacks of cytotoxicity on human gingival fibroblasts under our experimental conditions. This innovative composite material can even fight potential reinfections after endodontic treatment. Although we report promising data, additional experiments are needed to demonstrate the efficiency and safety of MTA-BisBAL NPs in patients with endodontic procedures over the long-term.

ACKNOWLEDGMENTS

Claudio Cabral-Romero wants to thank to CONACyT for financing the project 183825. Shankar Chellam was partially funded by the Texas Hazardous Waste Research Center. Also, Casiano Del Angel-Mosqueda wants to thank to CONACyT for his scholarship. All authors are grateful with Ismael Malagón Santiago for his help in the statistical analysis and Higinio Arzate from UNAM for providing HGF.

REFERENCES

1) Al-Hezaimi K, Al-Shalan TA, Naghshbandi J, Simon JH, Rotstein I. MTA preparations from different origins may vary in their antimicrobial activity. Oral Surg Oral Med Oral Pathol Oral Radiol Endod 2009; 107: e85-88.
2) Sarkar NK, Caicedo R, Ritwik P, Moiseyeva R, Kawashima I. Physicochemical basis of the biologic properties of mineral trioxide aggregate. J Endod 2005; 31: 97-100.
3) Parirokh M, Torabinejad M. Mineral trioxide aggregate: a comprehensive literature review—Part I: chemical, physical, and antibacterial properties. J Endod 2010; 36: 16-27.
4) England CG, Ng CF, Berkel VV, Frieboes HB. A review of pharmacological treatment options for lung cancer: Emphasis on novel nanotherapeutics and associated toxicity. Curr Drug Targets 2015; 16: 1057-1087.
5) Khan ST, Musarrat J, Al-Khedhairy AA. Countering drug

resistance, infectious diseases, and sepsis using metal and metal oxides nanoparticles: Current status. Colloids Surf B Biointerfaces 2016; 146: 70-83.
6) Favi PM, Gao M, Johana Sepulveda Arango L, Ospina SP, Morales M, Pavon JJ, Webster TJ. Shape and surface effects on the cytotoxicity of nanoparticles: Gold nanospheres versus gold nanostars. J Biomed Mater Res A 2015; 103: 3449-3462.
7) Norman NC. Chemistry of Arsenic, Antimony, and Bismuth. London, UK: Blackie Academic & Professional; 1998. 467 p.
8) Kotani T, Nagai D, Asahi K, Suzuki H, Yamao F, Kataoka N, Yagura, T. Antibacterial properties of some cyclic organobismuth (III) compounds. Antimicrob Agents Chemother 2005; 49: 2729-2734.
9) Badireddy AR, Chellam S. Antibacterial and antifouling properties of lipophilic bismuth compounds. In: Taylor JC, ed. Bismuth: Occurrence, Uses and Health & Environmental Effects. Advances in Chemistry Research. Vol 21. NY: Nova publishers; 2014.
10) Domenico P, Salo RJ, Novick SG, Schoch PE, Van Horn K, Cunha BA. Enhancement of bismuth antibacterial activity with lipophilic thiol chelators. Antimicrob Agents Chemother 1997; 41: 1697-1703.
11) Domenico P, Baldassarri L, Schoch PE, Kaehler K, Sasatsu M, Cunha BA. Activities of bismuth thiols against staphylococci and staphylococcal biofilms. Antimicrob Agents Chemother 2001; 45: 1417-1421.
12) Wu CL, Domenico P, Hassett DJ, Beveridge TJ, Hauser AR, Kazzaz JA. Subinhibitory bismuth-thiols reduce virulence of Pseudomonas aeruginosa. Am J Respir Cell Mol Biol 2002; 26: 731-738.
13) Huang CT, Stewart PS. Reduction of polysaccharide production in Pseudomonas aeruginosa biofilms by bismuth dimercaprol (BisBAL) treatment. J Antimicrob Chemother 1999; 44: 601-605.
14) Badireddy AR, Chellam S, Yanina S, Gassman P, Rosso KM. Bismuth dimercaptopropanol (BisBAL) inhibits the expression of extracelular polysaccharides and proteins in Brevundimonas doiminuta: implications for membrane microfiltration. Biotechnol Bioeng 2007; 99: 634-643.
15) Badireddy A, Hernandez-Delgadillo R, Sánchez-Nájera RI, Chellam S, Cabral-Romero C. Synthesis and characterization of lipophilic bismuth dimercaptopropanol nanoparticles and their effects on oral microorganisms growth and biofilm formation. J Nanopart Res 2014; 16: 1-12.
16) Hernandez-Delgadillo R, Badireddy AR, Zaragoza-Magaña V, Sánchez-Nájera RI, Chellam S, Cabral-Romero C. Effect of bismuth lipophilic nanoparticles (BisBAL NPs) on Erythrocytes. J Nanomater 2015; 2015: 1-15.
17) Hernandez-Delgadillo R, Badireddy AR, Martínez-Sanmiguel JJ, Contreras-Cordero JF, Martinez-Gonzalez GI, Sánchez-Nájera RI, Chellam S, Cabral-Romero C. Cytotoxic Effect of lipophilic bismuth dimercaptopropanol nanoparticles on epithelial cells. J Nanosci Nanotechnol 2016; 16: 203-209.
18) Tsaur SM, Chang SC, Luh KT, Hsieh WC. Antimicrobial susceptibility of enterococci in vitro. J Formos Med Assoc 1993; 92: 547-552.
19) Shokouhinejad N, Jafargholizadeh L, Khoshkhounejad M, Nekoofar MH, Raoof M. Surface microhardness of three thicknesses of mineral trioxide aggregate in different setting conditions. Restor Dent Endod 2014; 39: 253-257.
20) Ballester-Palacios ML, Berastegui-Jimeno EM, Parellada-Esquius N, Canalda-Sahli C. Interferometric microscopy study of the surface roughness of Portland cement under the action of different irrigants. Med Oral Patol Oral Cir Bucal 2013; 18: e817-821.
21) Carmona-Rodriguez B, Alvarez-Perez MA, Narayanan AS, Zeichner-David M, Reyes-Gasga J, Molina-Guarneros J, Garcia-Hernandez AL, Suarez-Franco JL, Chavarria IG, Villarreal-Ramirez E, Arzate H. Human cementum protein 1 induces expression of bone and cementum proteins by human gingival fibroblasts. Biochem Biophys Res Commun 2007; 358: 763-769.
22) Larsson R, Nygren P. A rapid fluorometric method for semiautomated determination of cytotoxicity and cellular proliferation of human tumor cell lines in microculture. Anticancer Res 1989; 9: 1111-1119.
23) Badireddy AR, Marinakos SM, Chellam S, Wiesner MR. Lipophilic nano-bismuth inhibits bacterial growth, attachment, and biofilm formation. Surf Innov 2013; 1: 181-189.
24) Swain P, Nayak SK, Sasmal A, Behera T, Barik SK, Swain SK, Mishra SS, Sen AK, Das JK, Jayasankar P. Antimicrobial activity of metal based nanoparticles against microbes associated with diseases in aquaculture. World J Microbiol Biotechnol 2014; 30: 2491-2502.
25) Song F, Li X, Wang Q, Liao L, Zhang C. Nanocomposite hydrogels and their applications in drug delivery and tissue engineering. J Biomed Nanotechnol 2015; 11: 40-52.
26) Samiei M, Farjami A, Dizaj SM, Lotfipour F. Nanoparticles for antimicrobial purposes in Endodontics: A systematic review of in vitro studies. Mater Sci Eng C Mater Biol Appl 2016; 58: 1269-1278.
27) Li F, Wang P, Weir MD, Fouad AF, Xu HH. Evaluation of antibacterial and remineralizing nanocomposite and adhesive in rat tooth cavity model. Acta Biomater 2014; 10: 2804-2813.
28) Lohbauer U, Wagner A, Belli R, Stoetzel C, Hilpert A, Kurland HD, Grabow J, Muller FA. Zirconia nanoparticles prepared by laser vaporization as fillers for dental adhesives. Acta Biomater 2010; 6: 4539-4546.
29) Estrela C, Bammann LL, Estrela CR, Silva RS, Pecora JD. Antimicrobial and chemical study of MTA, Portland cement, calcium hydroxide paste, Sealapex and Dycal. Braz Dent J 2000; 11: 3-9.
30) Tanomaru JM, Tanomaru-Filho M, Hotta J, Watanabe E, Ito IY. Antimicrobial activity of endodontic sealers based on calcium hydroxide and MTA. Acta Odontol Latinoam 2008; 21: 147-151.
31) Del Carpio-Perochena A, Kishen A, Shrestha A, Bramante CM. Antibacterial properties associated with chitosan nanoparticle treatment on root dentin and 2 types of endodontic Sealers. J Endod 2015; 41: 1353-1358.
32) Wang X, Wang B, Wang Y. Antibacterial orthodontic cement to combat biofilm and white spot lesions. Am J Orthod Dentofacial Orthop 2015; 148: 974-981.
33) Brennan SA, Ni Fhoghlu C, Devitt BM, O'Mahony FJ, Brabazon D, Walsh A. Silver nanoparticles and their orthopaedic applications. Bone Joint J 2015; 97-B: 582-589.
34) Siqueira PC, Magalhaes AP, Pires WC, Pereira FC, Silveira-Lacerda EP, Carriao MS, Bakuzis AF, Souza-Costa CA, Lopes LG, Estrela C. Cytotoxicity of glass ionomer cements containing silver nanoparticles. J Clin Exp Dent 2015; 7: e622-627.
35) Dawood AE, Manton DJ, Parashos P, Wong R, Palamara J, Stanton DP, Reynolds EC. The physical properties and ion release of CPP-ACP-modified calcium silicate-based cements. Aust Dent J 2015; 60: 434-444.
36) Malhotra N, Agarwal A, Mala K. Mineral trioxide aggregate: a review of physical properties. Compend Contin Educ Dent 2013; 34: e25-32.
37) Poggio C, Ceci M, Beltrami R, Dagna A, Colombo M, Chiesa M. Biocompatibility of a new pulp capping cement. Ann Stomatol 2014; 5: 69-76.